PARTICLE SEGREGATION IN GAS-SOLID FLUIDIZED BEDS WITH BINARY MIXTURES USING A MULTI-FLUID MODEL

Albert BOKKERS, Martin VAN SINT ANNALAND and Hans KUIPERS

Dept. Science and Technology, University of Twente, 7500 AE Enschede, THE NETHERLANDS

ABSTRACT

A Multi-Fluid Model (MFM) for the description of particle mixing and segregation in multi-disperse gas-solid fluidised beds was developed based on the kinetic theory of granular flow for multi-component systems. Several authors have derived or used a MFM assuming the particle velocities to be (at least close to) Maxwellian distributed around different mean velocities and with different granular temperatures for all particle species involved. However, this appears to be inconsistent with the first (equilibrium) approximation obtained from the Chapman-Enskog procedure. Therefore, a new set of closure equations for the rheologic properties of multi-component mixtures of slightly inelastic spherical particles has been derived using the Chapman-Enskog solution procedure of successive approximations, expanding the work of López de Haro et al. (1983) and Jenkins and Mancini (1989). In this theory the particle velocity distributions of all particle species are assumed to be (close to) Maxwellian distributed around the particle mixture velocity with the particle mixture granular temperature. Hence, particle segregation and differences in granular temperatures between different particle phases result from the first order perturbation function.

The new MFM closures have been implemented in an in-house numerical code. Segregation rates for a binary particle mixture in a freely bubbling gas-solid fluidised bed computed with the new MFM have been compared with experimental data obtained by Goldschmidt (2001). The computed degree of segregation as a function of time compare well with the experimental observations. However, the new MFM seems to underestimate the segregation rates at longer times (in strong contrast to other MFMs that strongly overestimate the segregation rates). This is most probably related to the neglect of frictional stresses associated with long-term, multiple particle-particle contacts resulting in an overestimation of the mobility of the emulsion phase.

NOMENCLATURE

a *Sonine coefficient*

b *Sonine coefficient*

$\overline{c}$ particle velocity, m/s

$\overline{C}$ peculiar velocity, m/s

$\overline{\mathbb{C}}$ dimensionless peculiar velocity, -

d *Sonine coefficient*

$\overline{d}$ *diffusion force, N*

e normal restitution coefficient, -

f particle velocity distribution, s^6/m^3

$\overline{F}$ external force, N/m^3

g radial distribution function, -

$\overline{g}$ gravity, m/s^2

h Sonine coefficient; vertical position, m

$\overline{\overline{I}}$ identity matrix

$\overline{J}$ diffusion mass flux, $kg/(m^2\,s)$

m particle mass, kg

n number density, $1/m^3$

N_p number of particle species, -

p pressure, Pa

$\overline{q}$ granular energy flux, $kg/(m\,s)$

$\overline{r}$ position, m

s relative segregation, -

S Sonine polynomial; actual segregation, -

t time, s

$\overline{u}$ ensemble averaged velocity, m/s

$\overline{v}$ diffusion velocity, m/s

x mass fraction, -

Greek symbols

β gas-particle drag, $kg/(m^3\,s)$

γ rate of granular energy dissipation due to particle-particle interactions, $kg/(m\,s^3)$

δ Kronecker delta

ε volume fraction, -

θ granular temperature, $kg\,m^2/s^2$

λ bulk viscosity, $kg/(m\,s)$

μ chemical potential, J; shear viscosity, $kg/(m\,s)$

ρ density, kg/m^3

σ particle diameter, m

$\overline{\overline{\tau}}$ stress tensor, Pa

ϕ particle quantity

subscripts

g gas phase

max   maximum

n, p particle phase n, p

s solids phase, particle mixture

superscripts

ex excess

$(0),(1)$ zero, first order Enskog approximation

INTRODUCTION

In many industrial dense gas-fluidised bed processes, like gas-phase polymerisation processes and granulation processes, mixtures of particles differing in size and/or density are encountered. In these processes, particle mixing and segregation phenomena play a very important role and determine the product quality to a large extent. Moreover, the continuous change in the particle size (and/or density) distribution due to granulation, affects the fluidisation behaviour of the bed. Bubbles are known to play an intricate and ambiguous role (Rowe and Nienow, 1976). On the one hand, rising bubbles can increase the particle segregation rates by carrying a mixture of particles to the top of the bed disturbing the local packing state of the bed, which might result in segregation of the larger or heavier particles. On the other hand, bubbles induce large scale mixing in the bed equalising the particle size/density distribution. Accurate prediction of segregation is required to improve the design, operation and scale-up of gas-fluidised bed granulation processes. With better understanding and a quantitative description of particle mixing and segregation phenomena, the growth rate and segregation dynamics can be better tuned to improve the product quality.

In order to gain more insight in how the operating conditions influence the particle mixing and segregation rates and to elucidate the role of the bubbles, fundamental hydrodynamic models are required. To enable a quantitative description of particle mixing and segregation phenomena, it is essential that the bubbles and the bubble behaviour (bubble break-up and bubble coalescence) is resolved with sufficient accuracy. This entails that a sufficiently large part of the fluidised bed is modelled in order to capture the macro-scale particle motion in the fluidised bed, while still completely resolving the phenomena occurring at the scale of a single bubble. Due to the required size of the computational domain to study particle mixing and segregation phenomena, a continuum modelling approach is needed. Smaller systems could be simulated with more detailed discrete particle models, which can (or even should) be used to validate assumptions required in the continuum approach (see a.o. Hoomans et al., 1998, 2000; Goldschmidt et al., 2002; Bokkers et al., 2004b). However, for systems at engineering scale that capture the macro-scale circulation patterns, the required number of particles and the corresponding calculation times would definitely become prohibitive. With discrete particle simulations the importance of particle-particle collision parameters on the bubble dynamics and consequent segregation rates has been demonstrated.

In the continuum approach both the gas and particulate phases are described as interpenetrating continua. In the continuum approach only the ensemble averaged behaviour is considered of a group of particles, which should be sufficiently large in number to allow for a statistical description of the particle-particle interactions, but also sufficiently small to still resolve all the prevailing local phenomena. Poly-disperse particle mixtures can be described with multi-fluid continuum models, which divide the particle mixture in a discrete number of classes, for which different physical properties may be specified. The conservation equations employed are a generalisation of the Navier-Stokes equations for interpenetrating continua. Owing to the continuum representation of the particle mixture, multi-fluid continuum models require additional closure laws for the description of the rheology of the particulate suspension. Since accurate modelling of bubble dynamics is of crucial importance to capture segregation dynamics and bubble behaviour strongly depends on the amount of energy dissipated in particle-particle collisions, the closure laws should account for the effect of energy dissipation due to non-ideal particle-particle encounters. Closure laws derived from the Kinetic Theory of Granular Flow (KTGF) have significantly improved the description of the rheology of mono-disperse gas-fluidised beds (see for a critical comparison Patil et al., 2005a, 2005b).

Several authors (a.o. Manger, 1996; Mathiesen, 1997; Huilin et al., 2001; Ramahan et al., 2003) have recently worked on the derivation of constitutive relations for binary and multi-component particle mixtures, basically extending the classical kinetic theory for multi-component dense gas mixtures. In these derivations it is assumed that the particle velocities are (approximately) Maxwellian distributed around *different* mean velocities and with a *different* granular temperature for each particle species. However, according to the Chapman-Enskog solution procedure (Chapman and Cowling, 1970) the first approximation to the particle velocity distribution for each species should indeed satisfy a Maxwellian distribution, but the mean velocity and granular temperature in the first (equilibrium) approximation should be *the same* for all the particle species (see also Jenkins and Mancini, 1989). It was believed that this assumption in the theory might (to a large extent) have caused the far too high segregation rates predicted by the continuum models (see Goldschmidt, 2001). Therefore, a novel set of closure relations for multi-component mixtures of slightly inelastic granular materials was derived, extending the classical kinetic theory for dense gas multi-component mixtures to account for non-ideal particle-particle collisions as well as for gas-particle drag. The Chapman-Enskog solution method of successive approximations was used (Chapman and Cowling, 1970), following the work by López de Haro et al. (1983) and Jenkins and Mancini (1987, 1989).

In this paper, the multi-fluid model equations are shortly presented. Subsequently, simulation results on the segregation rates in a bi-disperse freely bubbling fluidised bed computed with the multi-fluid model using the new closure relations are compared with dedicated experimental results obtained by Goldschmidt (2001) and with simulation results using the closure relations derived by Manger (1996).

MULTI-FLUID MODEL

Model equations

The kinetic theory of granular flow of multi-component mixtures describes the mean and fluctuating motion of particles of all species (1.. N_p) based on the assumption that the velocity distribution $f_n(\overline{c}_n, \overline{r}, t)$ of individual particles of species n, among a large number $n_n d\overline{r}$ of particles within an ensemble of volume $d\overline{r}$, can be

represented by the distribution of their velocity points $\overline{c}_n$ in the velocity space. The number of particles of species n per unit volume and the ensemble average of a particle quantity ϕ_n are respectively defined by:

$$n_n = \int f_n(\overline{c}_n, \overline{r}, t) d\overline{c}_n \qquad (1)$$

$$<\phi_n> = \frac{1}{n_n} \int \phi_n f_n(\overline{c}_n, \overline{r}, t) d\overline{c}_n \qquad (2)$$

Defining the mean velocity $\overline{u}_n$ of particle species n as $<\overline{c}_n>$, the mass average mixture velocity $\overline{u}_s$ is given by:

$$\overline{u}_s = \frac{1}{\varepsilon_s \rho_s} \sum_{n=1}^{N_p} \varepsilon_n \rho_n \overline{u}_n \qquad (3)$$

where the particle number density n_s, total solids volume fraction ε_s and the mixture density ρ_s are defined as

$$n_s = \sum_{n=1}^{N_p} n_n \qquad (4)$$

$$\varepsilon_s = \sum_{n=1}^{N_p} \varepsilon_n \quad \text{with} \quad \varepsilon_n = n_n \frac{\pi \sigma_n^3}{6} \qquad (5)$$

$$\rho_s = \frac{1}{\varepsilon_s} \sum_{n=1}^{N_p} \varepsilon_n \rho_n \quad \text{with} \quad \rho_n = m_n \frac{6}{\pi \sigma_n^3} \qquad (6)$$

The actual particle velocity $\overline{c}_n$ is decomposed into the local mass average mixture velocity $\overline{u}_s$ and the peculiar velocity $\overline{C}_n$:

$$\overline{c}_n = \overline{u}_s + \overline{C}_n \qquad (7)$$

Associated with the random motion of the particles, the granular temperature and the diffusion velocity of species n are defined as:

$$\theta_n = \frac{1}{3} m_n <C_n^2> \qquad (8)$$

$$\overline{v}_n = <\overline{C}_n> = \overline{u}_n - \overline{u}_s \qquad (9)$$

from which the mixture granular temperature is obtained by

$$\theta_s = \frac{1}{n_s} \sum_{n=1}^{N_p} n_n \theta_n \qquad (10)$$

and the diffusion velocities naturally satisfies

$$\sum_{n=1}^{N_p} \varepsilon_n \rho_n \overline{v}_n = \overline{0} \qquad (11)$$

The kinetic theory accounts for two different transport mechanisms of particle properties. On the one hand particles can transport a property by carrying it during free flight between collisions (kinetic transport); on the other hand particle quantities can be transferred during a collision (collisional transport). Modelling these transport mechanisms for a particulate mixture results in a set of coupled integral-differential equations for the particle velocity distributions of each particle species, referred to as the generalised Boltzmann equation. Based on the generalised Boltzmann equation the ensemble average transport equation for a particle property, referred to as the Maxwell transport equation, can be derived, with which the conservation equations for mass, momentum and granular energy can eventually be obtained (see Table 1).

Table 1. Conservation equations

Species continuity equations:

$$\frac{\partial}{\partial t}(\varepsilon_n \rho_n) + \nabla \cdot \left[\overline{J}_n + \varepsilon_n \rho_n \overline{u}_s \right] = 0$$

$$(n = 1, 2, ..., N_p)$$

Mixture continuity equation:

$$\frac{\partial}{\partial t}(\varepsilon_s \rho_s) + \nabla \cdot (\varepsilon_s \rho_s \overline{u}_s) = 0$$

Mixture momentum equations:

$$\frac{\partial}{\partial t}(\varepsilon_s \rho_s \overline{u}_s) + \nabla \cdot (\varepsilon_s \rho_s \overline{u}_s \overline{u}_s) = -\varepsilon_s \nabla p_g - \nabla p_s$$

$$-\nabla \cdot \overline{\overline{\tau}}_s + \sum_{n=1}^{N_p} \beta_{ng}(\overline{u}_g - \overline{u}_n) + \varepsilon_s \rho_s \overline{g}$$

Mixture granular temperature equation:

$$\frac{3}{2}\left[\frac{\partial(n_s \theta_s)}{\partial t} + \nabla \cdot (n_s \theta_s \overline{u}_s) \right] = -\left(p_s \overline{\overline{I}} + \overline{\overline{\tau}}_s \right) : \nabla \overline{u}_s$$

$$-\nabla \cdot \overline{q}_s - \sum_{n=1}^{N_p} 3 \frac{\beta_{ng}}{m_n} \theta_n - \gamma_s$$

Solving the generalised Boltzmann equation using the Chapman-Enskog solution procedure of successive approximations (Chapman and Cowling, 1970) explicit expressions for the solids phase rheology (solids phase stress tensor) are derived in terms of the mixture velocity and the mixture granular temperature (see Table 2 and 3). To warrant consistency with irreversible thermodynamics the revised Enskog theory by Van Beijeren and Ernst (1973) was used, following López de Haro et al. (1983). Explicit expressions for the bracket integrals for hard spheres up to the third order approximation can be found in Ferziger and Kaper (1972) and López de Haro et al. (1983). The equations to calculate the radial distribution function and the matching equations for the chemical potential of a multi-component hard-sphere fluid have been listed in Table 4.

Table 2. Constitutive equations for the particulate phase n:

Diffusion flux:

$$\overline{J}_n^{(1)} = -\frac{\varepsilon_n \rho_n}{2n_s}\left[\sum_{\ell=1}^{N_p} d_{n,0}^{(\ell)}\overline{d}_\ell - a_0^{(n)}\nabla\ln\theta_s\right]$$

Solid phase pressure:

$$p_s^{(1)} = \theta_s\left(n_s + \frac{2\pi}{3}\sum_{n=1}^{N_p}\sum_{p=1}^{N_p} n_n n_p \sigma_{np}^3 \frac{1+e_{np}}{2}g_{np}\right)$$

Solids phase stress tensor:

$$\overline{\overline{\tau}}_s^{(1)} = -\left(\lambda_s^{(1)} - \frac{2}{3}\mu_s^{(1)}\right)(\nabla\cdot\overline{u}_s)\overline{\overline{I}} - \mu_s^{(1)}\left((\nabla\overline{u}_s) + (\nabla\overline{u}_s)^T\right)$$

Solids phase shear viscosity:

$$\mu_s^{(1)} = \frac{1}{2}\frac{\theta_s}{n_s}\sum_{n=1}^{N_p}\left(1 + \frac{8\pi}{15}\sum_{p=1}^{N_p} n_p \sigma_{np}^3 \frac{m_p}{m_n+m_p}\frac{1+e_{np}}{2}g_{np}\right)n_n b_0^{(n)} + \frac{4}{15}\sqrt{2\pi\theta_s}\sum_{n=1}^{N_p}\sum_{p=1}^{N_p} n_n n_p \sigma_{np}^4 \sqrt{\frac{m_n m_p}{m_n+m_p}}\frac{1+e_{np}}{2}g_{np}$$

Solids phase bulk viscosity:

$$\lambda_s^{(1)} = \frac{4\pi}{3}\frac{\theta_s}{n_s}\sum_{n=1}^{N_p}\sum_{p=1}^{N_p} n_n n_p \sigma_{np}^3 \frac{m_p}{m_n+m_p}\frac{1+e_{np}}{2}g_{np}h_1^{(n)} + \frac{4}{9}\sqrt{2\pi\theta_s}\sum_{n=1}^{N_p}\sum_{p=1}^{N_p} n_n n_p \sigma_{np}^4 \sqrt{\frac{m_n m_p}{m_n+m_p}}\frac{1+e_{np}}{2}g_{np}$$

Granular energy dissipation:

$$\gamma_s^{(1)} = \pi\theta_s\sum_{n=1}^{N_p}\sum_{p=1}^{N_p} n_n n_p \sigma_{np}^3 \frac{m_p}{m_n+m_p}\left(1-e_{np}^2\right)g_{np}\left[\frac{4}{\sigma_{np}}\left(\frac{(m_n+m_p)\theta_s}{2\pi m_n m_p}\right)^{\frac{1}{2}} - \nabla\cdot\overline{u}_s\right]$$

Granular energy flux:

$$\overline{q}_s^{(1)} = -\frac{5}{4}\frac{\theta_s}{n_s}\sum_{n=1}^{N_p}\left(1 + \frac{24\pi}{15}\sum_{p=1}^{N_p} n_p \sigma_{np}^3 \frac{m_n m_p}{(m_n+m_p)^2}\frac{1+e_{np}}{2}g_{np}\right)n_n\left(a_1^{(n)}\nabla\ln\theta_s - \sum_{i=1}^{N_p} d_{n,1}^{(i)}\overline{d}_i\right)$$

$$-\frac{4}{3}\theta_s\sum_{n=1}^{N_p}\sum_{p=1}^{N_p}\left(\frac{2\pi\theta_s m_n m_p}{m_n+m_p}\right)^{\frac{1}{2}}\frac{n_n n_p}{m_n+m_p}\sigma_{np}^4 \frac{1+e_{np}}{2}g_{np}\nabla\ln\theta_s$$

$$+\frac{2\pi}{3}\theta_s\sum_{n=1}^{N_p}\sum_{p=1}^{N_p} n_p \sigma_{np}^3\left(\frac{m_n-m_p}{m_n+m_p}\right)\frac{1+e_{np}}{2}g_{np}\frac{\overline{J}_n^{(1)}}{m_n} + \frac{5}{2}\theta_s\sum_{n=1}^{N_p}\left(1 + \frac{2\pi}{3}\sum_{p=1}^{N_p} n_p \sigma_{np}^3 \frac{1+e_{np}}{2}g_{np}\right)\frac{\overline{J}_n^{(1)}}{m_n}$$

Diffusion force:

$$\overline{d}_n = -\frac{\varepsilon_n \rho_n}{\varepsilon_s \rho_s n_s \theta_s}\left[\nabla p_s^{(0)} + \sum_{p=1}^{N_p}\left(\varepsilon_n \rho_n \frac{\overline{F}_{\overline{u},n}}{m_n} - \varepsilon_p \rho_p \frac{\overline{F}_{\overline{u},p}}{m_p}\right)\right]$$

$$+\frac{n_n}{n_s}\sum_{p=1}^{N_p}\left[\delta_{np} + \frac{4\pi}{3}\frac{m_n}{m_n+m_p}n_p \sigma_{np}^3 g_{np}\right]\nabla\ln\theta_s + \frac{n_n}{n_s\theta_s}\sum_{p=1}^{N_p}\left(\frac{\partial\mu_n}{\partial n_p}\right)_{\theta_s,n_{k\neq p}}\nabla n_p$$

External forces based on averaged velocities:

$$\overline{F}_{\overline{u},n} = \overline{g} - \frac{1}{\rho_n}\nabla p_g + \frac{\beta_{ng}}{n_n m_n}\left(\overline{u}_g - \overline{u}_n\right)$$

First order approximation for the particulate phase pressure:

$$p_s^{(0)} = \theta_s\left(n_s + \frac{2\pi}{3}\sum_{n=1}^{N_p}\sum_{p=1}^{N_p} n_n n_p \sigma_{np}^3 g_{np}\right)$$

Table 3. Sonine coefficients

$$K_n = 1 + \frac{8\pi}{5} \sum_{p=1}^{N_p} n_p \sigma_{np}^3 \frac{m_n m_p}{(m_n + m_p)^2} g_{np} \qquad\qquad K'_n = 1 + \frac{8\pi}{15} \sum_{p=1}^{N_p} n_p \sigma_{np}^3 \frac{m_p}{m_n + m_p} g_{np}$$

$$K''_n = 1 + \frac{4\pi}{3} \sum_{p=1}^{N_p} n_p \sigma_{np}^3 \frac{m_p}{m_n + m_p} g_{np} - \frac{p_s^{(0)}}{n_s \theta_s}$$

$$\Lambda_{np}^{qr} = g_{np} \frac{8}{75} \frac{\sqrt{m_n m_p}}{\theta_s} \left\{ \delta_{np} \sum_{\ell=1}^{N_p} \frac{n_n n_\ell}{n_s^2} \left[S_{3/2}^{(q)}(\overline{\mathbb{C}}_n^2)\overline{\mathbb{C}}_n, S_{3/2}^{(r)}(\overline{\mathbb{C}}_n^2)\overline{\mathbb{C}}_n \right]'_{n\ell} + \frac{n_n n_p}{n_s^2} \left[S_{3/2}^{(q)}(\overline{\mathbb{C}}_n^2)\overline{\mathbb{C}}_n, S_{3/2}^{(r)}(\overline{\mathbb{C}}_n^2)\overline{\mathbb{C}}_n \right]''_{np} \right\}$$

$$H_{np}^{qr} = g_{np} \frac{2}{5\theta_s} \left\{ \delta_{np} \sum_{\ell=1}^{N_p} \frac{n_n n_\ell}{n_s^2} \left[S_{5/2}^{(q)}(\overline{\mathbb{C}}_n^2)\overline{\mathbb{C}}_n^0 \overline{\mathbb{C}}_n, S_{5/2}^{(r)}(\overline{\mathbb{C}}_n^2)\overline{\mathbb{C}}_n^0 \overline{\mathbb{C}}_n \right]'_{n\ell} + \frac{n_n n_p}{n_s^2} \left[S_{5/2}^{(q)}(\overline{\mathbb{C}}_n^2)\overline{\mathbb{C}}_n^0 \overline{\mathbb{C}}_n, S_{5/2}^{(r)}(\overline{\mathbb{C}}_n^2)\overline{\mathbb{C}}_n^0 \overline{\mathbb{C}}_n \right]''_{np} \right\}$$

$$\Gamma_{np}^{qr} = g_{np} \left\{ \delta_{np} \sum_{\ell=1}^{N_p} \frac{n_n n_\ell}{n_s^2} \left[S_{1/2}^{(q)}(\overline{\mathbb{C}}_n^2), S_{1/2}^{(r)}(\overline{\mathbb{C}}_n^2) \right]'_{n\ell} + \frac{n_n n_p}{n_s^2} \left[S_{1/2}^{(q)}(\overline{\mathbb{C}}_n^2), S_{1/2}^{(r)}(\overline{\mathbb{C}}_n^2) \right]''_{np} \right\}$$

$$\Delta_{np}^{qr} = g_{np} \frac{\sqrt{m_n m_p}}{\theta_s} \left\{ \delta_{np} \sum_{\ell=1}^{N_p} \frac{n_n n_\ell}{n_s^2} \left[S_{3/2}^{(q)}(\overline{\mathbb{C}}_n^2)\overline{\mathbb{C}}_n, S_{3/2}^{(r)}(\overline{\mathbb{C}}_n^2)\overline{\mathbb{C}}_n \right]'_{n\ell} + \frac{n_n n_p}{n_s^2} \left[S_{3/2}^{(q)}(\overline{\mathbb{C}}_n^2)\overline{\mathbb{C}}_n, S_{3/2}^{(r)}(\overline{\mathbb{C}}_n^2)\overline{\mathbb{C}}_n \right]''_{np} \right\}$$

where the Sonine polynomials have been defined as: $S_m^{(n)}(x) = \sum_{p=0}^{n} (-x)^p \frac{(m+n)_{n-p}}{p!(n-p)!}$, and r_q denotes the product of

the q factors r, $r-1$, ..., $r-q+1$, having used the dimensionless peculiar velocity: $\overline{\mathbb{C}}_n = \sqrt{\frac{m_n}{2\theta_s}}\overline{C}_n$

Sonine coefficients $a_r^{(n)}$:

$$\sum_{p=1}^{N_p} \sum_{r=0}^{N-1} \Lambda_{np}^{qr} a_r^{(p)} = \frac{4}{5} \frac{n_n}{n_s} K_n \delta_{q1} \qquad\qquad (n = 1, 2, ..., N_p; q = 0, 1, ..., N\text{-}1)$$

$$\sum_{n=1}^{N_p} \frac{\varepsilon_n \rho_n}{\varepsilon_s \rho_s} a_0^{(n)} = 0 \qquad\qquad (n = 1; q = 0)$$

Sonine coefficients $b_r^{(n)}$:

$$\sum_{p=1}^{N_p} \sum_{r=0}^{N-1} H_{np}^{qr} b_r^{(p)} = \frac{2}{\theta_s} \frac{n_n}{n_s} K'_n \delta_{q0} \qquad\qquad (n = 1, 2, ..., N_p; q = 0, 1, ..., N\text{-}1)$$

Sonine coefficients $h_r^{(n)}$:

$$\sum_{p=1}^{N_p} \sum_{r=0}^{N-1} \Gamma_{np}^{qr} h_r^{(p)} = \frac{n_n}{n_s} K''_n \delta_{q1} \qquad\qquad (n = 1, 2, ..., N_p; q = 0, 1, ..., N\text{-}1)$$

$$\sum_{n=1}^{N_p} \frac{n_n}{n_s} h_1^{(n)} = 0 \qquad\qquad (n = 1; q = 1)$$

Sonine coefficients $d_{n,r}^{(i)}$:

$$\sum_{p=1}^{N_p} \sum_{r=0}^{N-1} \Delta_{np}^{qr} d_{p,r}^{(i)} = 3 \left(\delta_{ni} - \frac{\varepsilon_n \rho_n}{\varepsilon_s \rho_s} \right) \delta_{q0} \qquad\qquad (n = 1, 2, ..., N_p; q = 0, 1, ..., N\text{-}1; i = 1, 2, ..., N_p)$$

$$\sum_{n=1}^{N_p} \frac{\varepsilon_n \rho_n}{\varepsilon_s \rho_s} d_{n,0}^{(i)} = 0 \qquad\qquad (n = 1; q = 0; i = 1, 2, ..., N_p)$$

Table 4. Radial distribution function and chemical potential for multi-component hard-sphere systems

Radial distribution function for multi-component hard-sphere particle mixtures:

$$g_{np} = \frac{1}{1-\varepsilon_s} + \left(g_0 - \frac{1}{1-\varepsilon_s} \right) \frac{<\sigma^{(2)}>\sigma_n\sigma_p}{<\sigma^{(3)}>\sigma_{np}} \qquad \text{where} \ <\sigma^{(j)}> = \sum_{n=1}^{N_p} \frac{n_n}{n_s}\sigma_n^j \ \text{and} \ \sigma_{np} = \frac{1}{2}\left(\sigma_n+\sigma_p\right)$$

Radial distribution function for a mono-disperse hard-sphere fluid:

$$g_0\left(\varepsilon_s\right) = \frac{\displaystyle\sum_{j=0}^{8} c_j\varepsilon_s^j}{\left(1-\left(\dfrac{\varepsilon_s}{\varepsilon_s^{\max}}\right)^a\right)^b}$$

where in this work the coefficients derived by Song et al. (1988) have been used:

$\varepsilon_s^{\max}$ = 0.6435, a = 1, b = 0.76, c_0 = 1, c_1 = 1.3192, c_2 = 1.41872, c_3 = 0.94208, c_4 = 0.1381376, c_5 = -0.3659776, c_6 = -2.336768, c_7 = -1.9857408, c_8 = -7.5431936.

Chemical potential of species n in a hard-sphere mixture:

$$\mu_n = \theta_s \ln n_n + \theta_s \ln \Lambda_n^3 + \mu_n^{ex}$$

where Λ_n represents the De Broglie wavelength for granular materials.

Excess chemical potential of species n:

$$\mu_n^{ex} = \theta_s y_n^{(3)} \left[\frac{1}{2}\left(m_1+m_2\right)4\varepsilon_s g_0 + \left(1+m_1-2m_2\right)\frac{\varepsilon_s}{1-\varepsilon_s} \right]$$

$$+ \frac{1}{2}\left[m_1\left(y_n^{(1)}+y_n^{(2)}-y_n^{(3)}\right)+m_2\left(3y_n^{(2)}-2y_n^{(3)}\right)\right]\theta_s \int_0^{\varepsilon_s} 4g_0(\varepsilon_s')d\varepsilon_s'$$

$$- \left[1+m_1\left(y_n^{(1)}+y_n^{(2)}-y_n^{(3)}\right)-2m_2\left(3y_n^{(2)}-2y_n^{(3)}\right)\right]\theta_s \ln\left(1-\varepsilon_s\right)$$

where $y_n^{(j)} = \dfrac{\sigma_n^j}{<\sigma^{(j)}>}$, $m_1 = \dfrac{<\sigma^{(1)}><\sigma^{(2)}>}{<\sigma^{(3)}>}$ and $m_2 = \dfrac{<\sigma^{(2)}>^3}{<\sigma^{(3)}>^2}$

It is important to note that in the Enskog solution procedure the first order approximation corresponds to the situation that the particulate suspension is in steady state and at equilibrium, i.e. the particles are not subjected to external forces, the particles are uniformly suspended (no gradients in solids volume fraction and velocity and granular energy) and that no kinetic energy is dissipated in the particle-particle collisions (e_{np} = 1). Thus, the first order approximation requires that the particle velocities of all particle species are distributed around *the same mean velocity* (the mixture velocity) with *the same granular temperature* (the mixture temperature). This is in contrast with the equations derived by Manger (1996), Mathiesen (1997), Huilin et al. (2001) and Ramahan et al. (2003), who assumed that the first order approximation to the particle velocity distribution is Maxwellian distributed around *different* mean velocities and *different* granular temperatures for all particle species involved. Hence, in this work differences in the granular temperatures for the different particle species and particle segregation are higher order effects arising from the first order perturbation function.

Numerical solution strategy

The Multi-Fluid model for a multi-disperse suspension consists of the total continuity and Navier-Stokes equations for the continuous gas phase and the species and mixture continuity equations, mixture Navier-Stokes equations and the mixture granular temperature equation for the solids phase. For the gas-particle drag the well-known closures by Ergun (1952) and Wen and Yu (1966) were used. Standard prescribed pressure, inflow, no slip and zero gradient boundary conditions were assumed in this work (see also Kuipers et al., 1992), since particle-wall collisions play a minor role in dense gas-fluidised beds. For dilute multi-disperse systems the boundary conditions proposed by Sinclair and Jackson (1989) could be extended.

A numerically advantageous feature of this Multi-Fluid model is that only the mixture Navier-Stokes equations and mixture granular temperature equation need to be solved, since explicit expressions have been derived for all the transport properties of the particulate phases in terms of the mixture velocity and the mixture granular temperature. This is in strong contrast to other Multi-Fluid models proposed in the literature (Manger, 1996; Mathiesen, 1997; Huilin et al., 2001; Ramahan et al., 2003), where Navier-Stokes equations and a granular temperature equation needs to be solved for every particle species present in the particulate mixture. The granular temperature and diffusion velocity of particle phase n can be directly computed from the mixture granular temperature, according to:

$$\theta_n^{(1)} = \theta_s \left(1 - \frac{h_1^{(n)}}{n_s} (\nabla \cdot \bar{u}_s) \right) \qquad (12)$$

$$\bar{v}_n = \bar{u}_n - \bar{u}_s = \frac{\overline{J}_n^{(1)}}{\varepsilon_n \rho_n} \qquad (13)$$

As a consequence of the first order perturbation function, particle phases of different diameter or density will in general possess different granular temperatures, which corresponds to experimental data by Zhang et al. (1996) for dilute gas-solid riser flow.

Due to the tendency of inelastic particles to contract into high-density clusters and the strong non-linearity of the particle pressure near the maximum packing density, special care is required in the numerical implementation of the Multi-Fluid model conservation equations.

The implementation is based on a finite difference technique employing a staggered grid and the numerical algorithm strongly resembles the Semi-Implicit Method for Pressure-Linked Equations (SIMPLE) described by Patankar and Spalding (1972). A detailed discussion on the application of this numerical technique to Two-Fluid models (TFM) for gas-solid fluidised beds has been presented by Kuipers et al. (1993). Basically, this method is a projection-correction method, which involves the solution of a Poisson equation for the gas phase pressure field to annihilate the mass residuals from the total gas phase continuity equation. In principle this numerical solution method can be applied straightforwardly to the Multi-Fluid model equations. However, due to the strong non-linear dependency of the solids phase pressure on the solids volume fraction, unacceptably small time steps are required in the order of magnitude of 10^{-5}-10^{-6} s.

Therefore, this numerical algorithm has been extended (see Goldschmidt, 2001) to directly take the compressibility of the particulate phase into account in the calculation of the particle volume fractions. In this numerical algorithm, referred to as the p-ε_s algorithm, an additional Poisson equation is solved (sequentially) for the total solids volume fraction field to minimise the mass residuals from the mixture solids phase continuity equation. Due to the enhanced numerical stability larger time steps can be handled (10^{-5}-10^{-4} s) with this method, even for strongly dissipative systems.

RESULTS

The particle segregation rates in a freely bubbling bi-disperse fluidised bed, consisting of a 25 % of 1.5 mm diameter (small) and 75 % of 2.5 mm diameter (large) glass beads (2526 kg/m³), computed by the Multi-Fluid Model, using a 45×120 grid, were compared with Digital Image Analysis (DIA) experiments performed by Goldschmidt (2001). In Figure 1 the evolution in time of the relative segregation is shown. The relative segregation s is defined for a binary mixture as:

$$s = \frac{S - 1}{S_{max} - 1} \qquad (14)$$

where $S = \frac{< h_{flotsam} >}{< h_{jetsam} >}$ and $S_{max} = \frac{2 - x_{flotsam}}{1 - x_{flotsam}}$

where $< h >$ and x represent the average vertical position and the mass fraction of the flotsam (the smaller/lighter particles) and jetsam (the bigger/heavier particles). The figure clearly shows that the MFM presented in this work no longer overestimates the particle segregation rate as was observed with the MFM proposed by Manger (1996). Using the MFM with the closures derived by Manger almost complete segregation is predicted within 15 s, in strong contrast to the experimental observations (only 60 % segregation after 60 s). Also Goldschmidt et al. (2001) and Huilin et al. (2003) showed that MFMs using the closure equations by Manger overpredicted the particle segregation rates of binary particle mixtures in freely bubbling fluidised beds. The segregation rates computed with the MFM developed in this work compare reasonably well with the experimentally observed segregation rates.
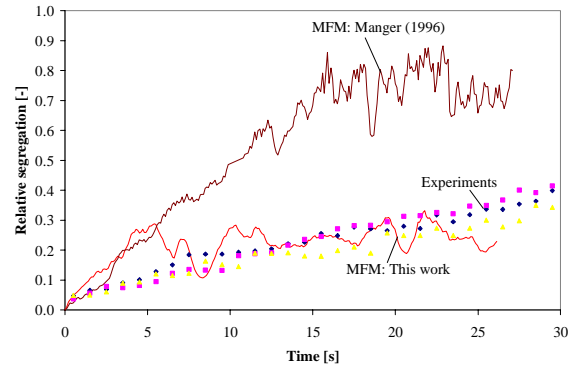

Figure 1. Relative segregation as a function of time in a freely bubbling bi-disperse fluidised bed consisting of 25% of 1.5 mm diameter and 75% 2.5 mm diameter glass beads (fluidization velocity: 1.20 m/s).

Snapshots of the flotsam fraction at different moments in time are given in Figure 2. The MFM with the new closure relations developed in this work predicts the build-up of a layer of flotsam on top of a mixed bed and a layer of jetsam at the bottom of the bed, as was also observed in the experiments. Remarkably, the MFM with the closure equations by Manger (1996) does not predict the formation of layer of smaller particles on top of a mixed bed; this model predicts that the particle segregation proceeds via 'sedimentation' of the heavier particles out of the particle mixture.
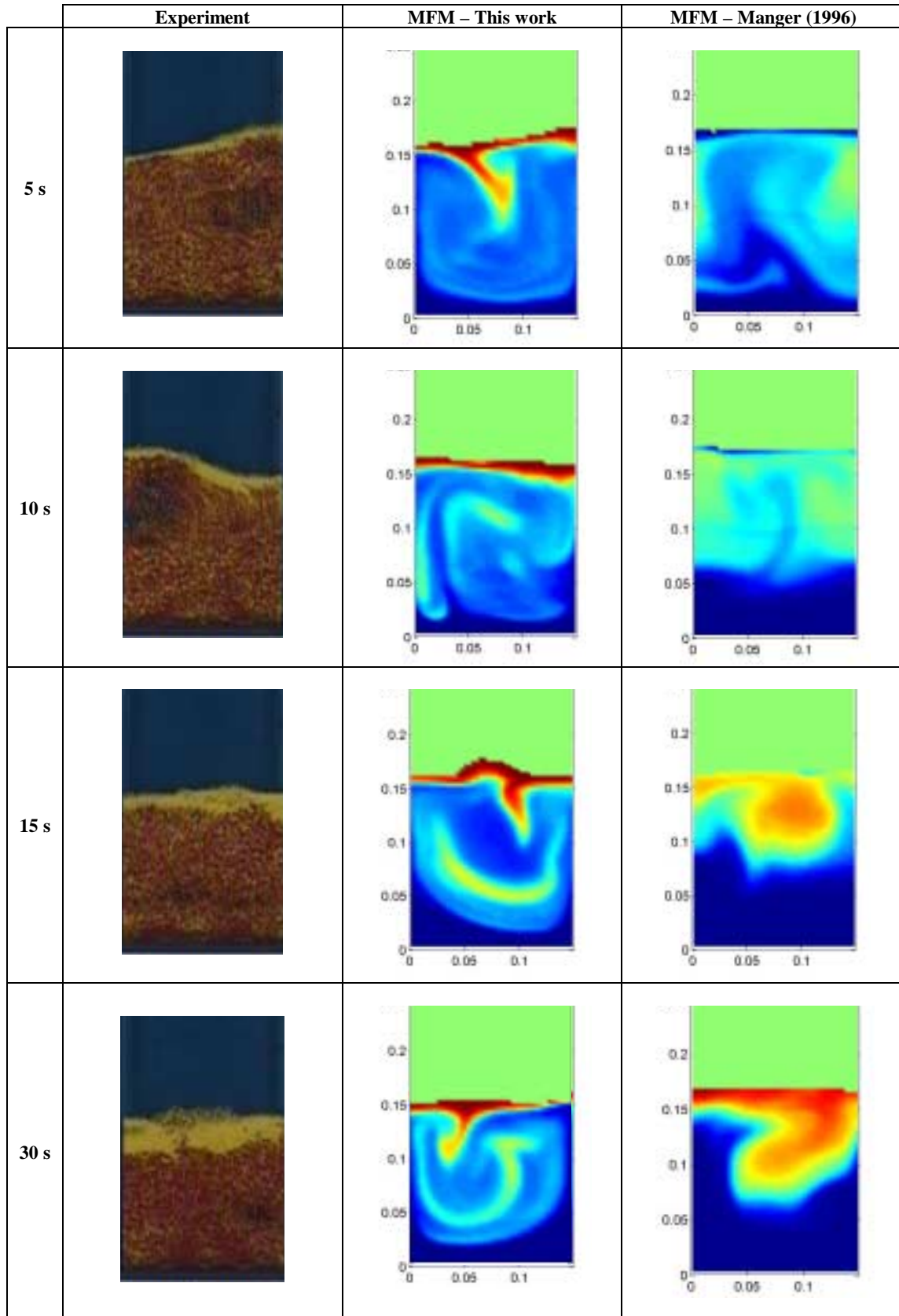
Figure 2. Plots of the flotsam fraction at different moments in time computed with the MFM presented in this work and the MFM proposed by Manger (1996) and compared with experimental results obtained by Goldschmidt (2001) for a freely bubbling bi-disperse fluidised bed consisting of 25% of 1.5 mm diameter (yellow) and 75% 2.5 mm diameter glass beads (red) (fluidization velocity: 1.20 m/s).

The MFM developed in this work seems to even underpredict the segregation rates, which can most probably be attributed to the neglect of frictional stresses associated with long-term multiple-particle contacts in the current implementation of the MFM. Due to the strong overestimation of the emulsion phase mobility, flotsam is continuously dragged downwards along the wall and jetsam is continuously dragged upwards in the centre of the bed due to the macro-scale circulation patterns in the fluidised bed induced by the bubbles. In both versions of the MFM, the one with Manger's closures and the one with the constitutive equations derived in this work, the frictional stresses were ignored and indeed the predicted emulsion phase mobility by both models was much too high in comparison with the experimental observations.

CONCLUSION

A Multi-Fluid Model based on the kinetic theory of granular flow for multi-component systems was developed using the Enskog solution method of successive approximations for the description of particle mixing and segregation in multi-disperse gas-solid fluidised beds. In this theory particle segregation and unequal granular temperatures in multi-disperse systems result from the first order perturbation function. Numerical simulations with the MFM have been compared with well-defined experiments performed by Goldschmidt (2001). The particle segregation rates computed with the new MFM compare much better with the experimental observations and are no longer overestimated, as was the case with MFMs presented before in the literature. Moreover, the formation of a flotsam and jetsam layer at the top and bottom of the bed is predicted correctly. However, due to the neglect of frictional stresses associated with long-term multiple particle-particle contacts, the emulsion phase mobility is strongly overestimated. Further developments in the description of frictional stresses are required to advance the continuum modelling of multi-disperse fluidised beds.

ACKNOWLEDGEMENTS

REFERENCES

BOKKERS, G.A., VAN SINT ANNALAND, M. and KUIPERS, J.A.M., (2004b), "Comparison of continuum models using the kinetic theory of granular flow with discrete particle models and experiments: extent of particle mixing induced by bubbles", in *Fluidization XI*, May 9-14, 2004, Naples, Italy, 187-194.

CHAPMAN, S. and COWLING, T.G., (1970), "The mathematical theory of non-uniform gases", 3rd ed., Cambridge university press, Cambridge, UK.

ERGUN, S. (1952), "Fluid flow through packed columns", *Chem. Engng Prog.*, **48**, 89-94.

FERZIGER, J.H. and KAPER, H.G., (1972), "Mathematical theory of transport processes in gases", North-Holland Pub. Co, Amsterdam, The Netherlands.

GOLDSCHMIDT, M.J.V., (2001), "Hydrodynamic modelling of fluidised bed spray granulation", Ph.D. Thesis, Enschede, The Netherlands.

GOLDSCHMIDT, M.J.V., KUIPERS, J.A.M., VAN SWAAIJ, W.P.M., (2001), "Hydrodynamic modelling of dense gas-fluidised beds using the kinetic theory of granular flow: effect of coefficient of restitution on bed dynamics", *Chem. Eng. Sci.*, **56**, 571-578.

GOLDSCHMIDT, M.J.V., BEETSTRA, R. and KUIPERS, J.A.M., (2002), "Hydrodynamic modelling of dense gas-fluidised beds: comparison of the kinetic theory of granular flow with 3D hard-sphere discrete particle simulations", *Chem. Eng. Sci.*, **57**, 2059-2075.

HOOMANS, B.P.B., KUIPERS, J.A.M., BRIELS, W.J. and VAN SWAAIJ, W.P.M., (1998). "Discrete particle simulation of segregation phenomena in dense gas-fluidized beds", in *Fluidization IX*, Eds. Fan, L.-S. and Knowlton, T.M., Engineering Foundation, New York, 485-492.

HOOMANS, B.P.B., KUIPERS, J.A.M. and VAN SWAAIJ, W.P.M., (2000). "Granular dynamics simulation of segregation phenomena in bubbling gas-fluidised beds", *Powder Technol.*, **109**, 41-48.

HUILIN, L., GIDASPOW, D. and MANGER, E., (2001), "Kinetic theory of fluidized binary granular mixtures", *Physical Review E*, **64**, 061301.

HUILIN, L., YURONG, H. and GIDASPOW, D., (2003), "Hydrodynamic modelling of binary mixture in a gas bubbling fluidized bed using the kinetic theory of granular flow.", *Chem. Eng. Sci.*, **58**, 1197-1205.

JENKINS, J.T. and MANCINI, F., (1987), "Balance laws and constitutive relations for plane flows of a dense, binary mixture of smooth, nearly elastic, circular discs", *J. Appl. Mech.*, **54**, 27-34.

JENKINS, J.T. and MANCINI, F., (1989), "Kinetic theory for binary mixtures of smooth, nearly elastic spheres", *Phys. Fluids A 1*, **12**, 2050-2057.

KOCH, D.L. and HILL, R.J., (2001), "Inertial effects in suspension and porous-media flows", *Annu. Rev. Fluid Mech.*, **33**, 619-647.

KUIPERS, J.A.M., VAN DUIN, K.J., VAN BECKUM, F.P.H. and VAN SWAAIJ, W.P.M., (1992), "A numerical model of gas-fluidized beds", *Chem. Eng. Sci.*, **47**, 1913-1924.

KUIPERS, J.A.M., VAN DUIN, K.J., VAN BECKUM, F.P.H. and VAN SWAAIJ, W.P.M., (1993), "Computer simulation of the hydrodynamics of a two-dimensional gas-fluidised bed", *Computers Chem. Eng.*, **8**, 839-858.

LOPEZ DE HARO, M., COHEN, E.G.D. and KINCAID, J.M., (1983), "Linear transport theory for multicomponent mixtures. I. Linear transport theory." *J. Chem. Phys.*, **78**, 2746-2759.

MANGER, E. (1996), "Modelling and simulation of gas/solids flow in curvilinear coordinates", Ph.D. Thesis, Telemark Institute of Technology, Porsgrunn, Norway.

MATHIESEN, V. (1997), "An experimental and computational study of multiphase flow behaviour in circulating fluidised beds", Ph.D. Thesis, Telemark Institute of Technology, Porsgrunn, Norway.

PATANKAR, S.V. and SPALDING, D.B., (1972), "A calculation procedure for heat, mass and momentum transfer in three dimensional parabolic flows", *Int. J. Heat Mass Transfer*, **15**, 1787-1806.

PATIL, D.J., VAN SINT ANNALAND, M. and KUIPERS, J.A.M., (2005a), "Critical comparison of hydrodynamic models for gas-solid fluidized beds: Part I – Bubbling gas-solid fluidized beds operated with a jet", *Chem. Eng. Sci.*, **60**, 57-72.

PATIL, D.J., VAN SINT ANNALAND, M. and KUIPERS, J.A.M., (2005b), "Critical comparison of hydrodynamic models for gas-solid fluidized beds: Part II – Freely bubbling gas-solid fluidized beds", *Chem. Eng. Sci.,* **60***,* 73-84.

RAMAHAN, M.F., NASER, J. and WITT, P.J., (2003), "An unequal granular temperature kinetic theory: description of granular flow with multiple particle classes", *Powder Technol.*, **138**, 82-92.

ROWE, P.N. and NIENOW, A.W., (1976), "Particle mixing and segregation in gas fluidised beds. A review", *Powder Technol.*, **15**, 141-147.

SINCLAIR, J.L. and JACKSON, R., (1989), "Gas-particle flow in a vertical pipe with particle-particle interactions", *AIChE J.*, **35**, 1473-1486.

SONG, Y., STRATT, R.M. and MASON, E.A., (1988), "The equation of state of hard spheres and the approach to random closest packing", *J. Chem. Phys.*, **88**, 1126-1133.

VAN BEIJEREN, H. and ERNST, M.H., (1973), "The modified enskog equation", *Physica*, **68**, 437-456.

WEN, Y.C. and YU, Y.H., (1966), "Mechanics of fluidization", *Chem. Eng. Prog. Symp. Ser.*, **62**, 100-111.

ZHANG, Y., YANG, Y. and ARASTAPOOR, H., (1996), "Electrostatic effect on the flow behaviour of a dilute gas/Cohesive particle flow system", *AIChE J.*, **42**, 159.